Web: www.witpress.com Email witpress@witpress.com
Paper from: *Damage and Fracture Mechanics VII*, CA Brebbia, & SI Nishida (Editors).
ISBN 1-85312-926-7

Effect of material conditions on structural integrity assessment

J. Vojvodič-Tuma[1], N. Gubeljak[2] & M. Oblak[2]
[1] *Institute for Metals and Technology, Ljubljana, Slovenia*
[2] *Faculty of Mechanical Engineering, University of Maribor, Smetanova 17, 2000 Maribor, Slovenia*

Abstract

High strength low alloy (HSLA) steels are used for the manufacturing of engineering structures (pipes, pressure vessels, cranes, off-shore structures, etc.), where they are exposed to different environmental influences and material ageing processes. Parts of the structures are also deformed during installation. However, the mechanical properties of steels change during manufacture and over their service lives. The consequences of this are changes in the resistance of steel in relation to ductile crack growth. The aim of this paper is to estimate the change in the ductile growth resistance of HSLA steels in relation to different supply conditions at room temperature and T_{NDT} temperatures and their effect on structure integrity assessment. The results show that decrease in mechanical properties and fracture toughness values contributed to higher risk of structure failure.

1 Introduction

According to structure integrity procedures [1, 2, 3], the fracture behavior of structure's materials depends on loading conditions, geometry of component and material properties. Therefore, in those cases when loading conditions and geometry of component are known, the material should ensure the integrity of the structures. The problem becomes serious if the materials properties change during manufacturing, installation or service. This can lead to unpredictable structure materials' failure. Hence, it is necessary to estimate the effect of different supply conditions on structural integrity.

Paper from: *Damage and Fracture Mechanics VII*, CA Brebbia, & SI Nishida (Editors).
ISBN 1-85312-926-7

In this paper the effect of three different supply conditions on High Strength Low Alloy (HSLA) steel were estimated for structure integrity, according to the SINTAP procedure [3].

2 Material

Observations of the yield strength and temperature effect on ductile crack growth resistance were made on High Strength Low Alloy-HSLA steel with the following chemical composition, table 1.

Table 1: Chemical compositions (weight %) of steel

C	Si	Mn	P	S	Cr	Ni	Mo	Nb	V	Al
0.19	0.42	1.49	0.013	0.005	0.13	0.10	0.04	0.050	0.07	0.087

Three different material conditions were observed:

a) HSLA steel in normalized condition (as-delivered), design »A«
b) Aged state, after 10% cool plastic deformation and heating at 250°C for 30 minutes, design »B«,
c) Deformed state after a 10% cool plastic deformation, design »C«.

The longitudinal tensile specimens, drop weight test and compact tension (CT) specimens were cut from a 20 mm thickness plate. The mechanical properties were determined at room temperature and at T_{NDT} temperatures (determined by drop weight testing) and by longitudinal testing, as given in Table 2. The increasing strength of the steel, associated with decreasing elongation at the fracture is clearly seen in Table 2. In addition, a further increase of yield strength with decrease of temperatures is obvious.

Table 2: Mechanical properties of both steels (V and C) at room temperature and T_{NDT} temperatures

Material condition	Yield Strength MPa	Ultimate Tensile Strength MPa	Elongation at fracture %	T_{NDT} °C	Yield strength at T_{NDT} MPa
VA	442	610	13.7	-72	514
VB	647	726	4.7	-104	780
VC	627	684	4.5	-134	757

Paper from: *Damage and Fracture Mechanics VII*, CA Brebbia, & SI Nishida (Editors).
ISBN 1-85312-926-7

3 Fracture toughness testing

On the basis of the results obtained (table 2), it was decided that fracture toughness testing would be carried out at room (+20°C) temperature and T_{NDT} temperatures.

Experiments were done on 6 series of 15 standard CT specimens. On the basis of the F-CMOD (Load versus Crack Mouth Opening Displacement) records, J-R resistance curves were determined, at room temperature and with J_c values at T_{NDT} temperatures (where all specimens were fractured in a brittle manner).
The parameters $J_{0.2BL}$ and J_c (determined from brittle fracture tests at T_{NDT}) were used for probabilistic analyses.

The widths of the confidence intervals for R=99% (at room and T_{NDT} temperatures) were determined by applying log-normal distribution law [4]. The results are listed in table 3.

Table 3: Widths of intervals ($J_{0.2BL}$ and J_c) and expected values at room temperature and T_{NDT} temperatures

Material condition	Toughness parameter $J_{0.2BL}$ N/mm			Toughness parameter J_c N/mm		
	Lower bound	Expected value	Upper bound	Lower bound	Expected value	Upper bound
A	420.5	476.5	532.5	3.31	52.62	102.1
B	209.4	231.6	253.8	1.23	20.44	40.1
C	297.9	333.2	368.4	3.85	25.02	46.1

4 Prediction of failure point by SINTAP procedure

The SINTAP procedure [3] is alternatively based on a Failure Assessment Diagram (FAD) or on a Crack Driving Force (CDF) philosophy [2]. When applying the FAD philosophy a failure line is constructed by normalizing the crack tip loading by the material's fracture resistance. The assessment of the component is then based on the relative location of a geometrically dependent assessment point with respect to this failure line. In the simplest application the component is regarded as safe as long as the assessment point lies within the area enclosed by the failure line. It is potentially unsafe if it is located on or above the failure line. If the crack tip loading is less than the fracture resistance the component is safe, otherwise it is potentially unsafe, as shown in Figure 1.
In the FAD route (Figure 1) a failure assessment curve (FAC), K_r versus L_r, is described by the equation

$$K_r = f(L_r) \tag{1}$$

Paper from: *Damage and Fracture Mechanics VII*, CA Brebbia, & SI Nishida (Editors).
ISBN 1-85312-926-7

To assess crack initiation and growth, two parameters need to be calculated. The first one K_r is defined by

$$K_r = \frac{K_I(a,F)}{K_{mat}} \tag{2}$$

where $K_I(a,F)$ is the linear-elastic stress intensity factor of the defective component and K_{mat} is fracture toughness, calculated by

$$K_{mat} = \sqrt{J \cdot E'} \tag{3}$$

with E' being Young's modulus E in plane stress (at RT) and $E/(1-\nu^2)$ in plane stress (at T_{NDT}). The quantity ν is Poisson's ratio.

The second parameter L_r is defined by:

$$L_r = \frac{F}{F_y} = \frac{p}{p_y} \tag{4}$$

where F_Y is the yield load or yield pressure p_Y of the cracked component.
The curve for assessment acceptability is calculated using the follow expression for those materials which have continued transition from elastic to plastic tensile behavior

$$f(L_r) = \left[1 + \frac{1}{2}L_r^2\right]^{-1/2} \cdot \left[0.3 + 0.7e^{-\mu L_r^6}\right] \quad \text{for } 0 \le L_r \le 1 \tag{5}$$

$$\text{where are } \mu = \min\begin{cases} 0.001E / R_{p0.2} \\ 0.6 \end{cases} \tag{6}$$

$$\text{and } f(L_r) = f(L_r = 1) \cdot L_r^{(N-1)/2N} \quad \text{for } 1 \le L_r \le L_{r\max} \tag{7}$$

The index of deformation hardening is given by the empirical expression

$$N = 0.3\left[1 + \frac{R_{p0.2}}{R_m}\right] \tag{8}$$

Plastic collapse is expected under the following conditions.

$$L_r^{\max} = \frac{1}{2}\left[\frac{R_{p0.2} + R_m}{R_{p0.2}}\right] \tag{9}$$

Paper from: *Damage and Fracture Mechanics VII*, CA Brebbia, & SI Nishida (Editors).
ISBN 1-85312-926-7

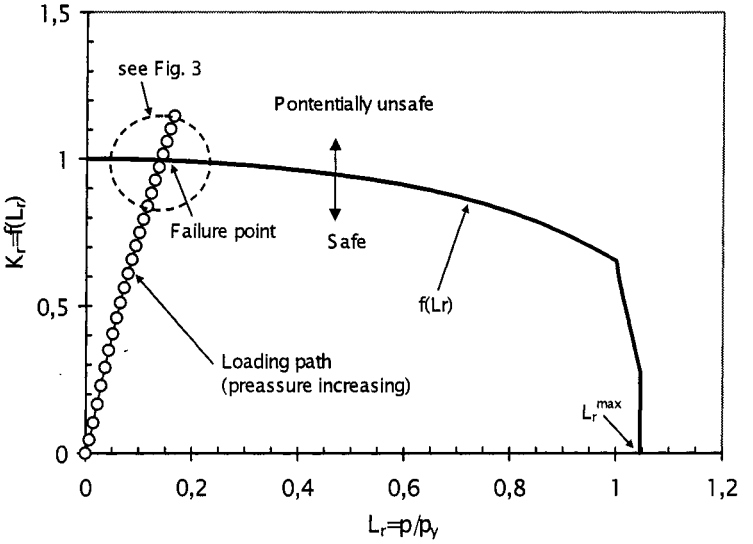

Figure 1: Determination of failure point by Failure Assessment Diagram-FAD

4.1 Structural integrity assessment of component

Since the service temperature can significantly change, it is necessary to estimate the effect of temperature decreasing on fracture behavior (from RT (ductile) to T_{NDT} (brittle) temperature) for the same crack length and configuration. In this case, a pipe under internal pressure p=250 bars (Figure 2.a, with outside diameter $2R_2$=525 mm, internal diameter $2R_1$=500 mm, wall thickness t=12.5 mm) was estimated. Calculation was performed for internal axial semi-elliptical surface crack, Figure 2.b. Two crack depths were estimated, with a=2.5 mm and a=7 mm with constant ratio between surface length 2c/a=10.

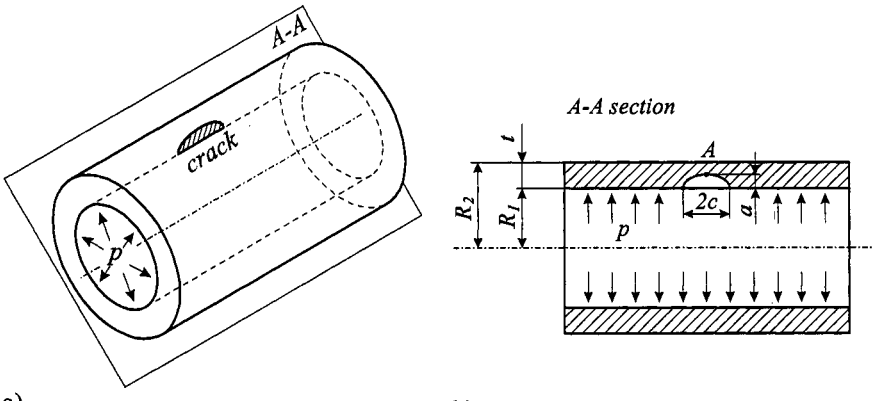

a) b)

Figure 2: Pipe with internal axial semi-elliptical surface defect

Paper from: *Damage and Fracture Mechanics VII*, CA Brebbia, & SI Nishida (Editors).
ISBN 1-85312-926-7

According to SINTAP [3] the stress intensity factor K_I is given by:

$$K_I = \sqrt{\pi \cdot a} \sum_{i=0}^{3} \sigma_i \cdot f_i\left(\frac{a}{t}, \frac{2c}{a}, \frac{R_1}{t}\right) \tag{10}$$

σ_i ($i=0$ *to* 3) are stress components which define the stress state s according to

$$\sigma = \sigma(u) = \sum_{i=0}^{3} \sigma_i \left(\frac{u}{a}\right)^i = \sigma_m + \sum_{i=1}^{3} \sigma_i \cdot \left(\frac{u}{a}\right)^i \qquad \text{for } 0 \le u \le a \tag{11}$$

u is defined as the co-ordinate at the centre of the elliptical crack. σ_m is membrane stress (normal to the perspective crack plane) in an un-cracked cylinder.

$$\sigma_m = \frac{p(R_2 + R_1)}{2 \cdot t} \tag{12}$$

σ_i ($i=1$ to 3) are in the absence of secondary stresses, equal to zero. Therefore, only the geometrical function f_i for $i=0$ was used for the deepest point of the crack (A) for $2c/a=10$ and $R_1/t=10$ ($f_0^A(a/t=0.2)=1.062$ and $f_0^A(a/t=0.56)=1.444$) in eq. (9).

Limit load solution for this working example is also given in SINTAP [3] by

$$p_Y = \frac{\sigma_Y}{(s+c)} \cdot \left[s \cdot \ln\left(\frac{R_2}{R_1}\right) + c\left(\frac{R_1}{R_1 + a}\right) \cdot \ln\left(\frac{R_2}{R_1 + a}\right) \right] \tag{13}$$

where

$$s = \frac{a \cdot c(1 - a/t)}{M \cdot R_1 \left[\ln\left(\frac{R_2}{R_1}\right) - \left(\frac{R_1}{R_1 + a}\right) \ln\left(\frac{R_2}{R_1 + a}\right) \right] - a} \tag{14}$$

and

$$M = \left(1 + \frac{1.61 \cdot c^2}{R_1 \cdot a}\right)^{0.5} \tag{15}$$

Solutions for a working example with constant internal pressure p=250 bars are shown in Figure 3. All ranges of fracture toughness values (with 99% reliability) at room temperature show low scatter within the safe area enclosed by the failure line. The assessment point in the case of ageing condition (noted by C) is shifted to lower loading capacity, in spite of higher yield strength. Additionally, ageing and deforming (noted by B) steel is shifted to lower bound capacity and potentially unsafe area at FAD. In the case of crack extension from a/t=0.2 to a/t=0.56 the assessment points on room temperature (RT) are shifted to a potentially unsafe area, too. The assessments points are completely changed with temperature decreasing at temperature T_{NDT}. At T_{NDT} temperature, especially both steel supply conditions (noted by B and C) are unsafe. These results are clearly shown in table 4, where "+" means safe and "–" potentially unsafe assessment points for the whole range of fracture toughness 99% probability.

Table 4 shows that with crack extension and at low temperature T_{NDT} the complete structure becomes unsafe. However, different supply conditions can at the same crack length and same temperature, reduce the safe service of a structure.

Paper from: *Damage and Fracture Mechanics VII*, CA Brebbia, & SI Nishida (Editors).
ISBN 1-85312-926-7

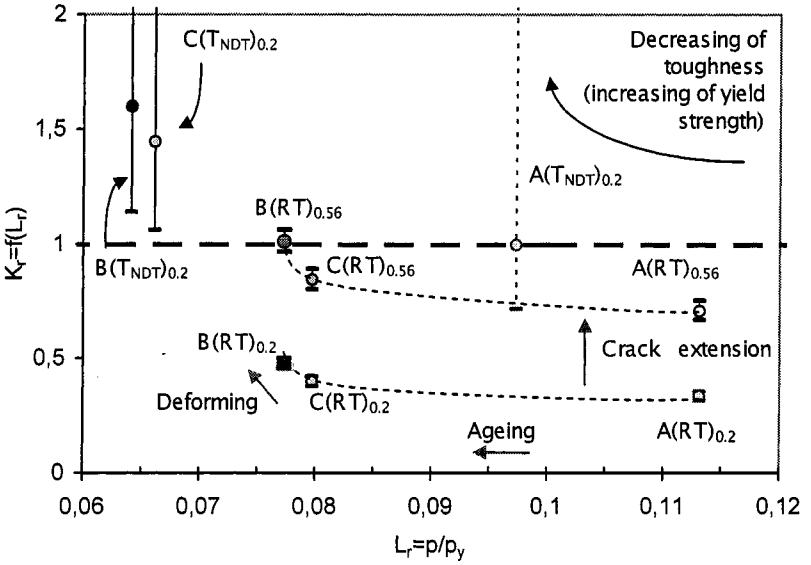

Figure 3: Effect of three different supply conditions of HSLA steel on structure integrity at room temperature (RT) and T_{NDT} temperatures (p=250 bars)

Table 4: Review of assessment points

Material	Toughness bound	a=2.5 mm 2c=25 mm		a=7 mm 2c=70 mm	
		RT	T_{NDT}	RT	T_{NDT}
VA	Lower	+	-	+	-
	Mean		+		
	Upper		+		
VB	Lower	+		-	-
	Mean		-	-	
	Upper			+	
VC	Lower	+		+	-
	Mean		-		
	Upper				
Effect of temperature		RT→T_{NDT}		RT→T_{NDT}	
Effect of crack growth		**a/t=0.2**		→	**a/t=0.56**

+ = safe; - = potentially unsafe

Paper from: *Damage and Fracture Mechanics VII*, CA Brebbia, & SI Nishida (Editors).
ISBN 1-85312-926-7

5 Conclusion

High Strength Low Alloy (HSLA) steel has higher resistance to ductile crack growth in the normalized (as-delivered) conditions at room temperature. Crack extension causes (vertical) shift to potentially unsafe areas in Failure Assessment diagram (FAD), meanwhile the ageing shifted (horizontally) to lower loading capacity. Aged and cold deformed steel is shifted to lower loading capacity and higher risk of failure, since yield strength is increasing whilst fracture toughness is decreasing. Decrease in temperature from RT to T_{NDT} caused higher risk of failure for all steel supply conditions. Since the fracture behavior on T_{NDT} is brittle and a range of 99% probability shows high scatter of assessment points, design against fracture is difficult.
Generally, in the case of cold-deformed or aged steel, the toughness of steel decreasing leads to decreasing of loading capacity and to potentially unsafe use of the structure.

Nomenclature

a	Crack length
c	Crack width
E	Young's modulus
E'	E in plane stress; $E/(1-\nu^2)$ in plane strain
K	Linear elastic stress intensity factor
K_{mat}	Crack fracture resistance in terms of critical K
K_r	Ration of applied K to the crack resistance, K/K_{mat}
L_r	Ratio of applied load, F, to yield load, F_Y
L_r^{max}	Plastic collapse limit of L_r
$R_{p0.2}$	Proof strength (materials without Lüders plateau)
R_m	Tensile strength (engineering)
ν	Poisson's ratio
σ_Y	Yield strength (general)

Reference:

[1] Kumar V., German M. D. and Shih C. F. (1981), An Engineering Approach for Elastic-Plastic Fracture Analysis, EPRI, Final Report to NP 1931
[2] R6 (1998): Assessment of the integrity of structures containing defects, Nuclear electric procedure R/H/R6, Revision 3
[3] SINTAP Procedure: Final version: November 1999
[4] Gubeljak N., Legat J., J. Vojvodic, Probabilistic Analyses of Yield Strength and Temperature Effects on the Ductile Crack Growth Resistance of HSLA Steels, ECF 10, Structural Integrity: Volume I, pp. 255-260, Berlin 1994